Journal of Sound and Vibration 332 (2013) 4339–4353

Contents lists available at SciVerse ScienceDirect

Journal of Sound and Vibration

journal homepage: www.elsevier.com/locate/jsvi

Modal structure of centrifugal pendulum vibration absorber systems with multiple cyclically symmetric groups of absorbers

Chengzhi Shi [a], Robert G. Parker [b,*]

[a] University of Michigan-Shanghai Jiao Tong University Joint Institute, Shanghai Jiao Tong University, Shanghai 200240, PR China
[b] Department of Mechanical Engineering, Virginia Tech, Blacksburg, VA 24061, USA

ARTICLE INFO

Article history:
Received 4 December 2012
Received in revised form
8 February 2013
Accepted 9 March 2013
Handling Editor: W. Lacarbonara
Available online 18 April 2013

ABSTRACT

This work studies the symmetry breaking effects on the vibration mode structure of centrifugal pendulum vibration absorber (CPVA) systems when multiple groups of absorbers are used. An absorber group is a set of equally spaced, identical absorbers. Absorbers within a group are cyclically symmetric while the entire system is asymmetric because the groups have no pre-defined relative angular spacing. One rotational and two translational degrees of freedom for the rotor and a single arclength degree of freedom for each absorber are considered in the planar model. The well-defined structure of the vibration modes is obtained by analytical and numerical investigations of the associated eigenvalue problem. This vibration mode structure is similar to that for CPVA systems with equally spaced, identical absorbers. Thus, the disrupted symmetry from multiple absorber groups does not destroy the vibration mode structure resulting from the cyclic symmetry within each group. The critical speeds and flutter instability of the system are investigated.

1. Introduction

Vibrations in rotating machinery can be counteracted by applying centrifugal pendulum vibration absorbers (CPVAs). They work because the absorber frequencies automatically adjust with the angular speed of the rotating device, and therefore to the dominant excitation frequencies. Thus, CPVA systems are order-tuned systems that counteract vibrations at a chosen order of rotation speed, not a fixed frequency.

In many applications all of the CPVAs are identical and equally spaced, but they can consist of multiple groups of absorbers tuned to different orders to counteract different harmonics of the vibrations. In rotating systems where the periodic torque excitation is non-sinusoidal, like the crankshafts of automotive engines, multiple harmonics of the excitation frequency excite the systems. When devices attached to the rotor have periodic features, such as pump vanes, compressors, and bladed components, they introduce additional excitation harmonics. Both cases can be counteracted by multiple groups of absorbers with different tuning orders. Helicopter rotors use absorbers to counteract translational (not rotational) displacements and require two different absorber groups [1]. Newly developed automotive engine technologies such as

* Corresponding author. Tel.: +1 540 231 6661; fax: +1 540 231 9364.
E-mail address: r.parker@vt.edu (R.G. Parker).

0022-460X/$ - see front matter © 2013 Elsevier Ltd. All rights reserved.
http://dx.doi.org/10.1016/j.jsv.2013.03.009

"multiple-displacement system" and "lugging" requires the use of multiple absorber groups that are tuned to different orders [2].

No work analyzes systems with multiple different groups of absorbers that are arbitrarily spaced relative to each other. Chao et al. investigated the unison [3] and non-unison dynamics [4] of multiple identical absorbers using the method of averaging and bifurcation theory. Shi and Parker [5] discovered the well-defined modal properties and stability conditions of cyclically symmetric (that is, identical and equally spaced) CPVA systems. Vidmar et al. [2] analyzed the nonlinear behavior of purely rotational, multiple order CPVA systems while the systems are cyclically symmetric. Multiple CPVAs with small imperfections have also been studied. For example, Chao and Shaw [6] used the method of averaging and group theory to analyze multiple pairs of torsional vibration absorbers with small imperfections in the paths of the absorbers. In other studies, Alsuwaiyan and Shaw discussed steady-state responses [7] and localization of free vibration modes [8] of nearly identical torsional vibration absorbers, taking into consideration the imperfection caused by mistuning. The imperfections break the symmetry of the CPVA systems, but only slightly. The use of multiple different groups of absorbers with arbitrary relative spacing between groups as studied in this work breaks the symmetry more severely. The question arises whether this symmetry breaking destroys the special modal properties possessed by cyclically symmetric CPVA systems.

The CPVA system contains a rotor and multiple absorber groups. The absorbers in each group are equally spaced and identical. Similar to the models in the studies of the engine shake problem by Cronin [9], helicopter rotor problem by Bauchau et al. [10], and cyclically symmetric CPVA systems [5], the rotor translational degrees of freedom are considered in this work.

After defining the CPVA system model, the linearized equations of motion for single-group systems derived in [5] are extended to multiple groups of absorbers. The vibration mode structure is first identified numerically, and only rotational, translational, and absorber modes are found. This structure is then proved analytically. The similarity of the vibration mode structure with that derived in [5] indicates that, surprisingly, the well-defined modal properties of identical, equally spaced systems persist despite the apparent symmetry breaking from the multiple groups of absorbers.

2. Mathematical model

The bifilar CPVAs [11–13] are considered as point masses. The inertia of the rollers used to suspend the absorbers [14] is neglected. Each group of CPVAs contains equally spaced, identical absorbers. The absorber groups have different numbers of absorbers, mass, distance of the pivots from the rotor axis, and pendulum radius relative to the pivot. While spacing within a group is equal, the spacing between different groups is arbitrary. Thus, the absorbers in one group are cyclically symmetric, but the entire system is not. Fig. 1 shows a CPVA system with two groups of absorbers. The first and second groups have four and five equally spaced, identical absorbers.

2.1. System parameters and bases

The system model consists of one rotor with p groups of absorbers mounted on it. Each group contains N_g absorbers, where $g=1,2,\ldots,p$, respectively. The rotor has two translational and one rotational degree of freedom. The mass and moment of inertia of the rotor are m_r and J_r. The translational stiffness of the rotor bearings is denoted by k_r. The mass of each absorber in the gth group is m_g. Dimensions l_g and r_g (Fig. 2) denote the distance between the center of the rotor and the pivot and the radius for each absorber, respectively. The tuning order of the gth group is $n_g=\sqrt{l_g/r_g}$.

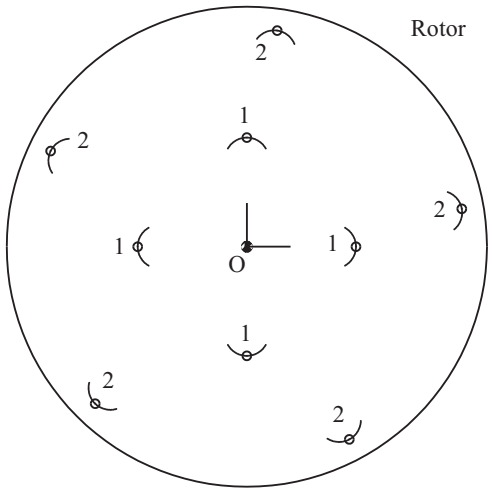

Fig. 1. Two groups of absorbers assembled with the rotor. 1 and 2 denote the absorbers belonging to the first and second groups, respectively.

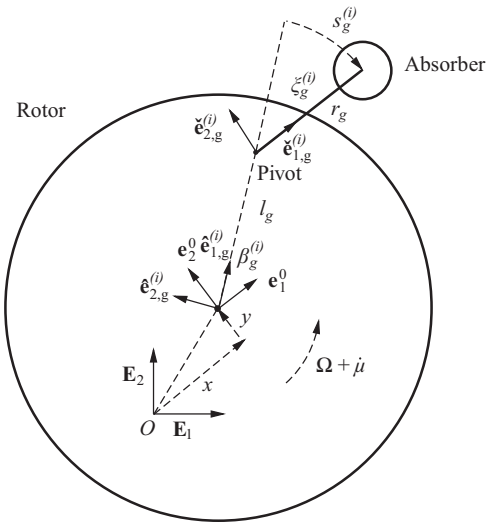

Fig. 2. Bases and coordinates used in the CPVA systems.

Fig. 2 shows the bases and coordinates used. $\{\mathbf{E}_1,\mathbf{E}_2\}$ is the fixed basis. $\{\mathbf{e}_1^0,\mathbf{e}_2^0\}$ corotates with the rotor at the nominal rotor speed Ω. Coordinates x and y denote the rotor translational vibrations along $\mathbf{e}_1^0$ and $\mathbf{e}_2^0$, respectively. The rotor rotational vibration is denoted by μ. The rotor-fixed basis $\{\hat{\mathbf{e}}_{1,g}^{(i)},\hat{\mathbf{e}}_{2,g}^{(i)}\}$ is assigned such that $\hat{\mathbf{e}}_{1,g}^{(i)}$ points from the center of the rotor to the pivot of the ith absorber in the gth group; angle $\beta_g^{(i)}$ describes its pivot position relative to $\{\mathbf{e}_1^0,\mathbf{e}_2^0\}$. The arclength coordinate $s_g^{(i)}=r_g\xi_g^{(i)}$ is the absorber deviation from the nominal position ($\xi_g^{(i)}=0$) for locally circular paths such as circular, cycloidal, and epicycloidal paths. The absorber-fixed basis $\{\hat{\mathbf{e}}_{1,g}^{(i)},\hat{\mathbf{e}}_{2,g}^{(i)}\}$ is shown in Fig. 2.,

2.2. Equations of motion and eigenvalue problem

The linearized equations of motion and generalized coordinate vector are

$$\mathbf{M}\ddot{\mathbf{q}}+\Omega\mathbf{G}\dot{\mathbf{q}}+(\mathbf{K}_b-\Omega^2\mathbf{K}_\Omega)\mathbf{q}=\mathbf{F}+\mathbf{H}. \tag{1a}$$

$$\mathbf{q}=(\mathbf{q}_r,\mathbf{q}_1,\mathbf{q}_2,\ldots,\mathbf{q}_p)^T, \tag{1b}$$

$$\mathbf{q}_r=(x,y,\mu)^T,\quad \mathbf{q}_g=(s_g^{(1)},s_g^{(2)},\ldots,s_g^{(N_g)})^T,\quad g=1,2,\ldots,p. \tag{1c}$$

Because the absorbers are not identical, adjustments are needed compared to the mass matrix $\mathbf{M}$, the gyroscopic matrix $\mathbf{G}$, and the stiffness matrices $\mathbf{K}_b$ and $\mathbf{K}_\Omega$ in [5] for cyclically symmetric systems. For the present case, these are

$$\mathbf{M}=\begin{pmatrix} \mathbf{M}_r & \mathbf{M}_{ra}^{(1)} & \mathbf{M}_{ra}^{(2)} & \cdots & \mathbf{M}_{ra}^{(p)} \\ & \mathbf{M}_a^{(1)} & \mathbf{0}_{N_1\times N_2} & \cdots & \mathbf{0}_{N_1\times N_p} \\ & & \mathbf{M}_a^{(2)} & \cdots & \mathbf{0}_{N_2\times N_p} \\ & & & \ddots & \vdots \\ \text{symmetric} & & & & \mathbf{M}_a^{(p)} \end{pmatrix}, \tag{2a}$$

$$\mathbf{G}=2\begin{pmatrix} \mathbf{G}_r & \mathbf{G}_{ra}^{(1)} & \mathbf{G}_{ra}^{(2)} & \cdots & \mathbf{G}_{ra}^{(p)} \\ & \mathbf{0}_{N_1\times N_1} & \mathbf{0}_{N_1\times N_2} & \cdots & \mathbf{0}_{N_1\times N_p} \\ & & \mathbf{0}_{N_2\times N_2} & \cdots & \mathbf{0}_{N_2\times N_p} \\ & & & \ddots & \vdots \\ \text{skew-symmetric} & & & & \mathbf{0}_{N_p\times N_p} \end{pmatrix}, \tag{2b}$$

$$\mathbf{K}_b=\begin{pmatrix}\mathbf{K}_{rb} & \mathbf{0}_{3\times N_1} & \mathbf{0}_{3\times N_2} & \cdots & \mathbf{0}_{3\times N_p}\\ & \mathbf{0}_{N_1\times N_1} & \mathbf{0}_{N_1\times N_2} & \cdots & \mathbf{0}_{N_1\times N_p}\\ & & \mathbf{0}_{N_2\times N_2} & \cdots & \mathbf{0}_{N_2\times N_p}\\ & & & \ddots & \vdots\\ \text{symmetric} & & & & \mathbf{0}_{N_p\times N_p}\end{pmatrix}, \tag{2c}$$

$$\mathbf{K}_\Omega=\begin{pmatrix}\mathbf{K}_r & \mathbf{K}_{ra}^{(1)} & \mathbf{K}_{ra}^{(2)} & \cdots & \mathbf{K}_{ra}^{(p)}\\ & \mathbf{K}_a^{(1)} & \mathbf{0}_{N_1\times N_2} & \cdots & \mathbf{0}_{N_1\times N_p}\\ & & \mathbf{K}_a^{(2)} & \cdots & \mathbf{0}_{N_2\times N_p}\\ & & & \ddots & \vdots\\ \text{symmetric} & & & & \mathbf{K}_a^{(p)}\end{pmatrix}, \tag{2d}$$

where the sub-matrices for $g=1,2,\ldots,p$ are

$$\mathbf{M}_r=\begin{pmatrix}m_r+\sum_{g=1}^{p}N_g m_g & 0 & -\sum_{g=1}^{p}m_g(l_g+r_g)\sum_{i=1}^{N_g}\sin\beta_g^{(i)}\\ & m_r+\sum_{g=1}^{p}N_g m_g & \sum_{g=1}^{p}m_g(l_g+r_g)\sum_{i=1}^{N_g}\cos\beta_g^{(i)}\\ \text{symmetric} & & J_r+\sum_{g=1}^{p}N_g m_g(l_g+r_g)^2\end{pmatrix}, \tag{3a}$$

$$\mathbf{M}_{ra}^{(g)}=\begin{pmatrix}-m_g\sin\beta_g^{(1)} & -m_g\sin\beta_g^{(2)} & \cdots & -m_g\sin\beta_g^{(N_g)}\\ m_g\cos\beta_g^{(1)} & m_g\cos\beta_g^{(2)} & \cdots & m_g\cos\beta_g^{(N_g)}\\ m_g(l_g+r_g) & m_g(l_g+r_g) & \cdots & m_g(l_g+r_g)\end{pmatrix}, \tag{3b}$$

$$\mathbf{M}_a^{(g)}=\operatorname{diag}(\underbrace{m_g,m_g,\cdots,m_g}_{N_g}), \tag{3c}$$

$$\mathbf{G}_r=\begin{pmatrix}0 & -(m_r+\sum_{g=1}^{p}N_g m_g) & -\sum_{g=1}^{p}m_g(l_g+r_g)\sum_{i=1}^{N_g}\cos\beta_g^{(i)}\\ & 0 & -\sum_{g=1}^{p}m_g(l_g+r_g)\sum_{i=1}^{N_g}\sin\beta_g^{(i)}\\ \text{skew-symmetric} & & 0\end{pmatrix}, \tag{3d}$$

$$\mathbf{G}_{ra}^{(g)}=\begin{pmatrix}-m_g\cos\beta_g^{(1)} & -m_g\cos\beta_g^{(2)} & \cdots & -m_g\cos\beta_g^{(N_g)}\\ -m_g\sin\beta_g^{(1)} & -m_g\sin\beta_g^{(2)} & \cdots & -m_g\sin\beta_g^{(N_g)}\\ 0 & 0 & \cdots & 0\end{pmatrix}, \tag{3e}$$

$$\mathbf{K}_{rb}=\operatorname{diag}(k_r,k_r,0), \tag{3f}$$

$$\mathbf{K}_r=\operatorname{diag}\left(m_r+\sum_{g=1}^{p}N_g m_g,m_r+\sum_{g=1}^{p}N_g m_g,0\right), \tag{3g}$$

$$\mathbf{K}_{ra}^{(g)}=\begin{pmatrix}-m_g\sin\beta_g^{(1)} & -m_g\sin\beta_g^{(2)} & \cdots & -m_g\sin\beta_g^{(N_g)}\\ m_g\cos\beta_g^{(1)} & m_g\cos\beta_g^{(2)} & \cdots & m_g\cos\beta_g^{(N_g)}\\ 0 & 0 & \cdots & 0\end{pmatrix}, \tag{3h}$$

$$\mathbf{K}_a^{(g)}=\operatorname{diag}(\underbrace{-m_g l_g/r_g,-m_g l_g/r_g,\cdots,-m_g l_g/r_g}_{N_g}). \tag{3i}$$

F and **H** in Eq. (1a) are the external force and the constant centripetal acceleration term caused by the rotor speed, respectively. Their expressions are

$$\mathbf{F}=(F_x(t),F_y(t),T_r(t),\underbrace{0,0,\ldots,0}_{\sum_{g=1}^{p}N_g})^T, \tag{4a}$$

$$\mathbf{H}=\Omega^2\left(\sum_{g=1}^{p} m_g(l_g+r_g)\sum_{i=1}^{N_g}\cos\beta_g^{(i)},\ \sum_{g=1}^{p} m_g(l_g+r_g)\sum_{i=1}^{N_g}\sin\beta_g^{(i)},\underbrace{0,0,\ldots,0}_{\sum_{g=1}^{p}N_g+1}\right)^T, \tag{4b}$$

where $F_x(t)$, $F_y(t)$, and $T_r(t)$ denote the forces and torque applied to the rotor. $\mathbf{H}$ vanishes because the absorbers in each group are equally spaced, which gives $\sum_{i=1}^{N_g}\cos\beta_g^{(i)}=\sum_{i=1}^{N_g}\sin\beta_g^{(i)}=0$ for all $g=1,2,\ldots,p$ [5].

Substitution of $\mathbf{q}=\boldsymbol{\phi}e^{\lambda t}$ into Eq. (1a) yields

$$\lambda^2\mathbf{M}\boldsymbol{\phi}+\lambda\Omega\mathbf{G}\boldsymbol{\phi}+(\mathbf{K}_b-\Omega^2\mathbf{K}_\Omega)\boldsymbol{\phi}=\mathbf{0}, \tag{5}$$

which is a gyroscopic eigenvalue problem [15] whose eigenvalues and eigenvectors both appear as complex conjugate pairs. The eigenvalues of Eq. (5) are

$$\lambda_{1,2}=\frac{-\mathrm{j}\tilde{g}\pm\sqrt{-\tilde{g}^2-4\tilde{m}\tilde{k}}}{2\tilde{m}}, \tag{6}$$

where $\mathrm{j}=\sqrt{-1}$, $\tilde{m}=\overline{\boldsymbol{\phi}}^T\mathbf{M}\boldsymbol{\phi}$, $\mathrm{j}\tilde{g}=\Omega\overline{\boldsymbol{\phi}}^T\mathbf{G}\boldsymbol{\phi}$, and $\tilde{k}=\overline{\boldsymbol{\phi}}^T(\mathbf{K}_b-\Omega^2\mathbf{K}_\Omega)\boldsymbol{\phi}$ [5,16]. The scalars $\tilde{m}$, $\tilde{g}$, and $\tilde{k}$ are real. Based on this, one can show that both λ and $-\lambda$ are eigenvalues of Eq. (5), and so are λ and $\overline{\lambda}$ (where the overbar denotes the complex conjugate).

3. Vibration mode structure

The vibration mode structure of CPVA systems with multiple groups of absorbers is first identified by numerical solution of Eq. (5). The subsequent analytical derivations verify the numerical observations.

For reference, in cyclically symmetric CPVA systems the vibration mode structure consists of two pairs of complex conjugate rotational modes, four pairs of complex conjugate translational modes, and a pair of complex conjugate absorber modes with eigenvalue multiplicity $N-3$, where N is the number of absorbers [5].

3.1. Numerical approach

Figs. 3 and 4 show four of the vibration modes of the CPVA system with both the first (four absorbers) and second (five absorbers) groups described in Table 1. The arbitrarily chosen first absorbers of the two groups are separated by 10°. Only rotational modes (Fig. 3(a) and (b)), translational modes (Fig. 3(c) and (d)), and absorber modes (Fig. 4) exist in the system vibration mode structure. The various degrees of freedom are not in-phase, a consequence of the gyroscopic structure of Eq. (5) yielding complex-valued vibration modes. The rotor rotates without any translation for the rotational modes, and it translates without any rotation for the translational modes. No rotor motion (x,y,μ) exists in the absorber modes. For rotational modes, all absorbers in the same group vibrate identically and in-phase with each other, and 180° out-of-phase with the rotor rotation (Fig. 3(a) and (b)). For translational modes, the two rotor translational coordinates are equal in amplitude and 90° out-of-phase with each other. All absorbers in both groups have identical amplitude, and the phase angles are dictated by each absorber's angular location $\beta_g^{(i)}$ (Fig. 3(c) and (d)). Each absorber mode associates with a group of absorbers, and only that group moves (Fig. 4). For these modes, all absorbers have equal amplitude. The phase angles are dictated by $k\beta_g^{(i)}$, where the integer k is the phase index discussed later.

Table 2 shows the natural frequencies of two CPVA example systems with both of the first (four absorbers) and second (four absorbers) groups in Table 1 used. For convenience, the $\mathbf{e}_1^0$ axis is assigned such that it points from the center of the rotor to the pivot of one absorber. Here we define this absorber as the first absorber of the associated group and the nearest absorber belonging to another group in the counterclockwise direction as the first absorber of that other group. The spacing angle between these absorbers is defined as the relative spacing between the two groups. For the symmetric case stated in Table 2, the relative spacing between the two groups can be 0° or 45°; while here it is chosen to be 45°, these two relative spacing options yield the same natural frequencies. For the asymmetric case, the relative spacing can be chosen arbitrarily other than zero and 45°. The relative spacing between the two groups is 10° in Table 2. From Table 2, the numbers of modes in each of the three mode types and the natural frequencies of the symmetric and asymmetric systems are identical. In fact, the same result holds for arbitrary relative spacing between the two groups. The relative spacing between the groups does not affect the mode structure (number of modes of each type) or the natural frequencies. The specific modes can change, however, as discussed below.

Numerous numerical experiments show that the eigenvectors of the rotational and absorber modes remain identical when the spacing between the two groups defined above varies. Thus, the spacing angle between the two groups appears to have no effect on the rotational and absorber modes. The eigenvectors of the translational modes, however, are different when the relative spacing changes. The phase difference between the motions of the first absorbers in the two groups equals the relative spacing angle or this spacing angle plus 180° (see Fig. 3(d), for example, where the phase difference between s_1 and s_5 is 10°, which is the spacing angle between the two first absorbers). Phase angles of other absorbers also change based on relative spacing. Thus, only the translational mode eigenvectors (but not the eigenvalues) are affected by the group relative spacing, while all the other eigenvalues and eigenvectors of the system are independent of the relative spacing.

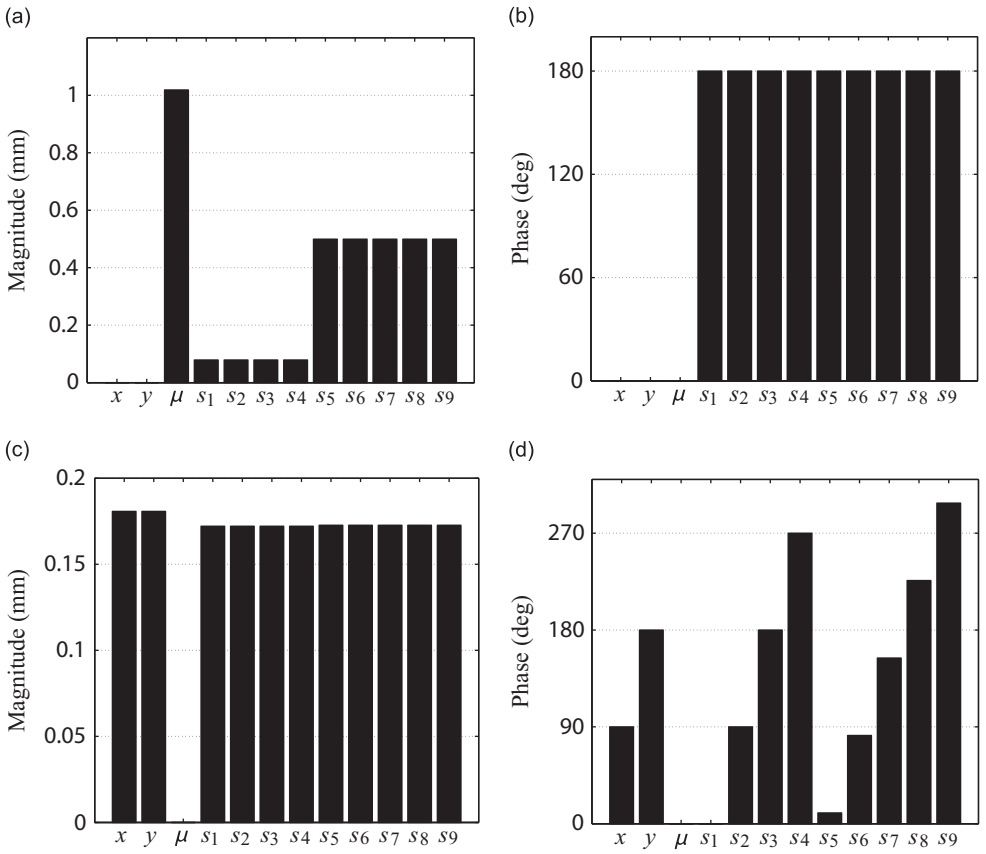

Fig. 3. Sample rotational and translational modes of the CPVA system with both of the first (four absorbers) and second (five absorbers) groups in Table 1 used at rotor speed $\Omega = 2000$ rpm (209.44 rad/s). The horizontal axis labels denote the system degrees of freedom. The two rotor translation and one rotor rotational degrees of freedom are denoted by x, y, and μ, respectively. The coordinates s_1 to s_4 denote the absorber motions in the first group, and s_5 to s_9 denote the absorber motions in the second group. The spacing between the first absorbers of the two groups is 10°. (a) Rotational mode magnitude, $\lambda = \mathrm{j}704.25$ rad/s; (b) rotational mode phase, $\lambda = \mathrm{j}704.25$ rad/s; (c) translational mode magnitude, $\lambda = \mathrm{j}8242.3$ rad/s; and (d) translational mode phase, $\lambda = \mathrm{j}8242.3$ rad/s.

Table 3 shows the vibration mode structures for the CPVA systems described with the parameters given by Table 1. For cases 1, 3, and 8 in Table 3, one can choose a suitable group relative spacing such that the system is cyclically symmetric (like the example discussed for Table 2 above). Cyclically symmetric cases (cases 1, 3, and 8) exist only when the number of absorbers in all groups is integer multiples of all the numbers of absorbers in groups having fewer absorbers (and no groups have only one absorber). Other relative spacing renders the system asymmetric (cases 2, 4, 5, 6, 7, and 9). As shown in Table 3 (cases 1, 2, 3, 4, 8, and 9), the relative spacing of the groups does not affect the number of modes in the three mode types. This matches the result of Table 2. The number of absorbers in the groups can be either even or odd. The combination of groups with even and odd numbers of absorbers shown in Table 3 (cases 5, 6, and 7) does not change the vibration mode structure either.

Generalizing, there are $p+1$ pairs of complex conjugate rotational modes, $2(p+1)$ pairs of complex conjugate translational modes, and p pairs of complex conjugate absorber modes. The eigenvalue multiplicity of the absorber modes associated with the gth group is N_g-3.

3.2. Rotational modes

From the foregoing numerical evidence, a general rotational mode eigenvector has the form

$$\boldsymbol{\phi} = (0,0,\mu,\underbrace{s_1,s_1,\ldots,s_1}_{N_1},\underbrace{s_2,s_2,\ldots,s_2}_{N_2},\ldots,\underbrace{s_p,s_p,\ldots,s_p}_{N_p})^T. \tag{7}$$

In such a mode, all absorbers within a given group have identical amplitude and phase. The absorber motions of different groups are coupled indirectly through the rotor rotation. Substitution of Eq. (7) into the eigenvalue problem in Eq. (5) and algebraic reduction yield the $(p+1)\times(p+1)$ self-adjoint, non-gyroscopic rotational mode eigenvalue problem as

$$\lambda^2\mathbf{M}^{(r)}\boldsymbol{\phi}^{(r)} + \Omega^2\mathbf{K}_{\Omega}^{(r)}\boldsymbol{\phi}^{(r)} = \mathbf{0}, \tag{8a}$$

$$\boldsymbol{\phi}^{(r)} = (\mu,s_1,s_2,\ldots,s_p)^T, \tag{8b}$$

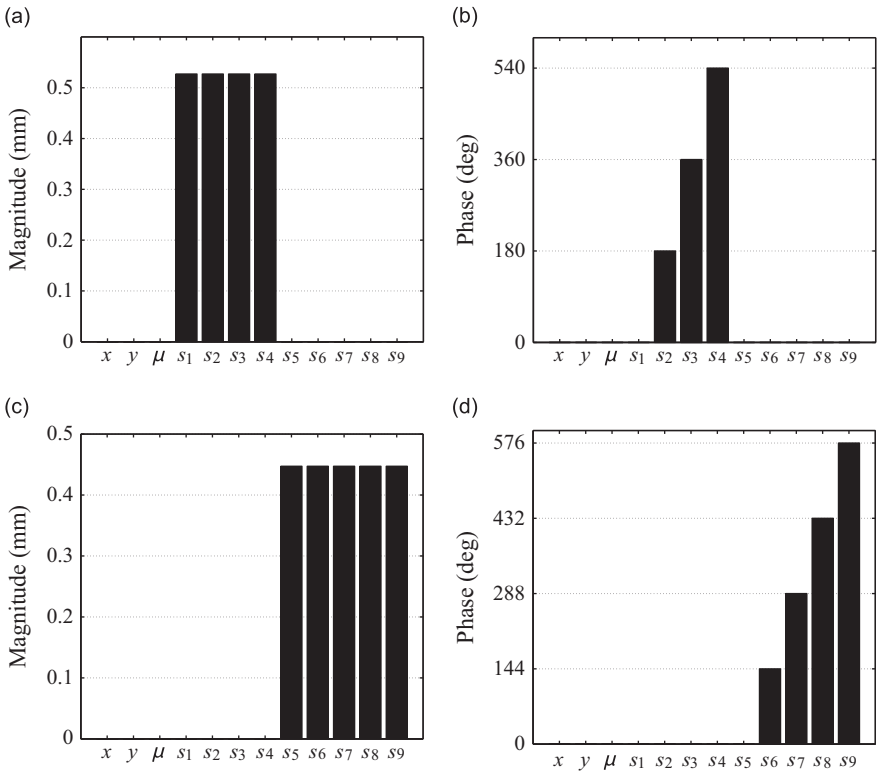

Fig. 4. Sample absorber modes of the CPVA system with both of the first (four absorbers) and second (five absorbers) groups in Table 1 used at rotor speed $\Omega = 2000$ rpm (209.44 rad/s). The horizontal axis labels denote the system degrees of freedom. The two rotor translation and one rotor rotational degrees of freedom are denoted by x, y, and μ, respectively. The coordinates s_1 to s_4 denote the absorber motions in the first group, and s_5 to s_9 denote the absorber motions in the second group. The spacing between the first absorbers of the two groups is 10°. (a) Absorber mode magnitude, $\lambda = \mathrm{j}418.88$ rad/s; (b) absorber mode phase, $\lambda = \mathrm{j}418.88$ rad/s; (c) absorber mode magnitude, $\lambda = \mathrm{j}628.32$ rad/s; and (d) absorber mode phase, $\lambda = \mathrm{j}628.32$ rad/s. The modes shown in this figure have phase index $k=2$.

Table 1
Parameters of CPVA example systems.

Parameter	First group	Second group	Third group
Rotor mass, m_r (kg)		11	
Rotor inertia, J_r (kg m^2)		0.2	
Rotor translational stiffness, k_r (N/m)		1×10^9	
Absorber mass, m (kg)	0.9	1	1.1
Distance between center and pivot, l (m)	0.04	0.09	0.16
Absorber radius, r (m)	0.01	0.01	0.01

Table 2
Natural frequencies, ω (rad/s), of the CPVA system with the first (four absorbers) and second (four absorbers) groups of Table 1 used at rotor speed $\Omega = 2000$ rpm (209.44 rad/s). The two groups of absorbers are equally spaced on the rotor for the equal spacing case. The first absorbers are placed 10° apart for the unequal spacing case.

Spacing	Rotational			Translational						Absorber	
Symmetric	0	425.70	689.83	418.54	418.87	627.53	628.27	8071.6	8381.9	418.88	628.32
Asymmetric	0	425.70	689.83	418.54	418.87	627.53	628.27	8071.6	8381.9	418.88	628.32

$$\mathbf{M}^{(r)} = \begin{pmatrix} J_r + \sum_{g=1}^{p} N_g m_g (l_g + r_g)^2 & N_1 m_1 (l_1 + r_1) & N_2 m_2 (l_2 + r_2) & \cdots & N_p m_p (l_p + r_p) \\ & N_1 m_1 & 0 & \cdots & 0 \\ & & N_2 m_2 & \cdots & 0 \\ & & & \ddots & \vdots \\ & \text{symmeteric} & & & N_p m_p \end{pmatrix}, \tag{8c}$$

Table 3
Numbers of rotational, translational, and absorber modes of CPVA example systems with multiple groups of absorbers at rotor speed $\Omega = 2000$ rpm (209.44 rad/s). The parameters are given in Table 1. The numbers of the absorber modes are shown as sums to indicate the relations between the absorber modes and their associated groups (the order of the sum corresponds to the numbering of the groups). Multiplicities are shown in parentheses.

Case number	Spacing between groups	Number of groups	Number of absorbers			Number of pairs		
			First group	Second group	Third group	Rotational	Translational	Absorber
1	Symmetric	2	4	4	N/A	3	6	1+1
2	Asymmetric	2	4	4	N/A	3	6	1+1
3	Symmetric	2	4	8	N/A	3	6	1+1(5)
4	Asymmetric	2	4	8	N/A	3	6	1+1(5)
5	Asymmetric	2	4	5	N/A	3	6	1+1(2)
6	Asymmetric	2	4	6	N/A	3	6	1+1(3)
7	Asymmetric	2	5	7	N/A	3	6	1(2)+1(4)
8	Symmetric	3	4	4	4	4	8	1+1+1
9	Asymmetric	3	4	4	4	4	8	1+1+1

$$\mathbf{K}_{\Omega}^{(t)} = \mathrm{diag}\left(0, N_1 m_1 \frac{l_1}{r_1}, N_2 m_2 \frac{l_2}{r_2}, \ldots, N_p m_p \frac{l_p}{r_p}\right). \tag{8d}$$

The two equations that govern the rotor translation in Eq. (5) vanish because $\sum_{i=1}^{N_g} \cos\beta_g^{(i)} = \sum_{i=1}^{N_g} \sin\beta_g^{(i)} = 0$, where $g = 1,2,\ldots,p$. Eq. (8) provides the $p+1$ pairs of complex conjugate eigensolutions that are substituted into Eq. (7) to get the $p+1$ pairs of complex conjugate rotational modes.

Because Eq. (8a) is self-adjoint, the rotational mode eigenvectors are real. The p absorber equations in Eq. (8) give

$$s_g = -\frac{\lambda^2 (l_g + r_g)}{\lambda^2 + (l_g/r_g)\Omega^2}\mu, \quad g = 1,2,\ldots,p. \tag{9}$$

For purely imaginary eigenvalues, coordinates μ and s_g are in-phase if $|\lambda^2| < (l_g/r_g)\Omega^2$, and 180° out-of-phase if $|\lambda^2| > (l_g/r_g)\Omega^2$ (see Fig. 3(b), where both groups in the system satisfy the second condition).

A rigid body mode $\boldsymbol{\phi}^{(r)} = (\mu, \underbrace{0,0,\ldots,0}_{p})^T$ with zero eigenvalue is one of the $p+1$ eigensolutions of Eq. (8).

According to Eq. (7), the absorbers in the same group move with identical magnitudes (Fig. 3(a)), and no phase differences exist between their motions (Fig. 3(b)). This is a standing wave mode [17]. The absorber motions in the gth group are

$$\boldsymbol{\phi}_g = s_g(\underbrace{1,1,\ldots,1}_{N_g})^T = s_g(e^{jk\beta_g^{(1)}}, e^{jk\beta_g^{(2)}}, \ldots, e^{jk\beta_g^{(N_g)}})^T. \tag{10}$$

The second equality in Eq. (10) is introduced to define the phase index k of a vibration mode [5,18]. For cyclically symmetric systems, this phase index is the factor multiplying the spacing angles in the exponential terms of Eq. (10). Here it controls the phase of the absorber motions. As seen in Eq. (10), the phase index of all rotational modes is zero, which is identical to that derived for cyclically symmetric CPVA systems [5].

3.3. Translational modes

The numerical experiments reveal the translational mode eigenvector as

$$\boldsymbol{\phi} = (\boldsymbol{\phi}_r, \boldsymbol{\phi}_1, \boldsymbol{\phi}_2, \ldots, \boldsymbol{\phi}_p)^T, \tag{11a}$$

$$\boldsymbol{\phi}_r = (x, jx, 0)^T \tag{11b}$$

$$\boldsymbol{\phi}_g = s_g(e^{j\beta_g^{(1)}}, e^{j\beta_g^{(2)}}, \ldots, e^{j\beta_g^{(N_g)}})^T, \quad g = 1,2,\ldots,p. \tag{11c}$$

According to Eq. (11), the motions of the absorbers in the gth group have equal magnitudes and relative phase difference of $360°/N_g$ between adjacent absorbers (Fig. 3(c) and (d)). This is a traveling wave mode [17]. The factor multiplying the spacing angles in the exponential terms of Eq. (11c) is unity, so the phase index of translational modes is $k=1$. The absorber motions of different groups are coupled indirectly through the rotor translation.

With the properties that $\sum_{i=1}^{N_g} e^{j\beta_g^{(i)}} \sin\beta_g^{(i)} = j(N_g/2)$ and $\sum_{i=1}^{N_g} e^{j\beta_g^{(i)}} \cos\beta_g^{(i)} = N_g/2$ for $g = 1,2,\ldots,p$ [5], substitution of Eq. (11) into Eq. (5) yields the $(p+1)\times(p+1)$ gyroscopic translational mode eigenvalue problem as

$$\lambda^2 \mathbf{M}^{(t)}\boldsymbol{\phi}^{(t)} + \lambda\Omega\mathbf{G}^{(t)}\boldsymbol{\phi}^{(t)} + (\mathbf{K}_b^{(t)} - \Omega^2\mathbf{K}_{\Omega}^{(t)})\boldsymbol{\phi}^{(t)} = \mathbf{0}, \tag{12a}$$

$$\boldsymbol{\phi}^{(t)} = (x, s_1, s_2, \ldots, s_p)^T, \tag{12b}$$

$$\mathbf{M}^{(t)} = \begin{pmatrix} 2\left(m_r + \sum_{g=1}^{p} N_g m_g\right) & -\mathrm{j}N_1 m_1 & -\mathrm{j}N_2 m_2 & \cdots & -\mathrm{j}N_p m_p \\ & N_1 m_1 & 0 & \cdots & 0 \\ & & N_2 m_2 & \cdots & 0 \\ & & & \ddots & \vdots \\ \text{Hermitian} & & & & N_p m_p \end{pmatrix}, \tag{12c}$$

$$\mathbf{G}^{(t)} = 2\begin{pmatrix} -2\mathrm{j}\left(m_r + \sum_{g=1}^{p} N_g m_g\right) & -N_1 m_1 & -N_2 m_2 & \cdots & -N_p m_p \\ & 0 & 0 & \cdots & 0 \\ & & 0 & \cdots & 0 \\ & & & \ddots & \vdots \\ \text{skew-Hermitian} & & & & 0 \end{pmatrix}, \tag{12d}$$

$$\mathbf{K}_b^{(t)} = \mathrm{diag}(2k_r, \underbrace{0,0,\ldots,0}_{p}), \tag{12e}$$

$$\mathbf{K}_\Omega^{(t)} = \begin{pmatrix} 2\left(m_r + \sum_{g=1}^{p} N_g m_g\right) & -\mathrm{j}N_1 m_1 & -\mathrm{j}N_2 m_2 & \cdots & -\mathrm{j}N_p m_p \\ & -N_1 m_1 \dfrac{l_1}{r_1} & 0 & \cdots & 0 \\ & & -N_2 m_2 \dfrac{l_2}{r_2} & \cdots & 0 \\ & & & \ddots & \vdots \\ \text{Hermitian} & & & & -N_p m_p \dfrac{l_p}{r_p} \end{pmatrix}. \tag{12f}$$

These matrices are complex. The equation that governs the rotor rotation in Eq. (5) vanishes for the same reason as for the rotor translation equations for rotational modes. The $2(p+1)$ eigensolutions provided by the translational mode eigenvalue problem in Eq. (12) with complex matrices are not complex conjugate pairs but rather distinct eigensolutions. Substitution of $\overline{\boldsymbol{\phi}}$ (with phase index $k=-1$ or equivalently N_g-1) into the equations of motion in Eq. (1) gives Eq. (12a) with all matrices replaced by their complex conjugate. This yields the complex conjugates of the $2(p+1)$ eigensolutions of Eq. (12a). Thus, $2(p+1)$ pairs of complex conjugate translational modes exist. The phase indices of translational modes are $k=\pm 1$, the same as for cyclically symmetric CPVA systems [5].

The p absorber equations in Eq. (12) yield

$$s_g = \mathrm{j}\frac{(\mathrm{j}\lambda+\Omega)^2}{\lambda^2+(l_g/r_g)\Omega^2}x, \quad g=1,2,\ldots,p. \tag{13}$$

For purely imaginary eigenvalues, the translational coordinate x and the first absorber coordinate of the gth group $s_g^{(1)}$ are $90^\circ+\beta_g^{(1)}$ (if $|\lambda^2|<(l_g/r_g)\Omega^2$) or $270^\circ+\beta_g^{(1)}$ (if $|\lambda^2|>(l_g/r_g)\Omega^2$) out-of-phase (see Fig. 3(d), where the system falls into the second category). The addition of $\beta_g^{(1)}$ is because of the phase difference between s_g and $s_g^{(1)}$ (the first element of $\boldsymbol{\phi}_g$) in Eq. (11c). These same phase relations exist for only one group of identical, equally spaced absorbers [5].

Based on Eq. (13) for imaginary λ, s_g and x are either 90° or 270° out-of-phase for every $g=1,2,\ldots,p$ depending on their tuning orders $n_g=l_g/r_g$. Thus, the s_g that describe the phases between the groups $g=1,2,\ldots,p$ are all either in-phase or 180° out-of-phase with each other. Hence, the phase angles of the absorber coordinates in Eq. (11c) are exactly determined by the angular positions $\beta_g^{(1)},\beta_g^{(2)},\ldots,\beta_g^{(N_g)}$ and the tuning order of each group (Fig. 3(d)).

In Fig. 3(c), the magnitudes of the coordinates of the two groups of absorbers are nearly identical. This is because the magnitude of the eigenvalue of this mode ($\lambda=\mathrm{j}8242.3$ rad/s) is much larger than the rotor speed ($\Omega=209.44$ rad/s). Thus, the second term in the denominator of Eq. (13) is negligible, and the magnitudes of the s_g are almost the same for all $g=1,2,\ldots,p$.

3.4. Absorber modes

The absorber mode eigenvector associated with the gth group is

$$\boldsymbol{\phi} = (0,0,0,\mathbf{0}_{1\times N_1},\mathbf{0}_{1\times N_2},\ldots,\mathbf{0}_{1\times N_{g-1}},\mathbf{s}_g,\mathbf{0}_{1\times N_{g+1}},\cdots,\mathbf{0}_{1\times N_p})^T, \tag{14a}$$

$$\mathbf{s}_g = (s_g^{(1)},s_g^{(2)},\ldots,s_g^{(N_g)})^T, \quad g=1,2,\ldots,p. \tag{14b}$$

Substitution of Eq. (14) into the absorber equations in Eq. (5) yields the absorber mode eigenvalues as

$$\lambda = \pm \mathrm{j}\Omega\sqrt{\frac{l_g}{r_g}} = \pm \mathrm{j}\Omega n_g. \tag{15}$$

Substitution of $\lambda = \mathrm{j}\Omega n_g$ into the three rotor equations in Eq. (5) gives

$$\mathbf{A}_g \mathbf{s}_g = \mathbf{0}, \tag{16a}$$

$$\mathbf{A}_g = \begin{pmatrix} 1 & 1 & \cdots & 1 \\ \mathrm{e}^{\mathrm{j}\beta_g^{(1)}} & \mathrm{e}^{\mathrm{j}\beta_g^{(2)}} & \cdots & \mathrm{e}^{\mathrm{j}\beta_g^{(N_g)}} \\ \mathrm{e}^{-\mathrm{j}\beta_g^{(1)}} & \mathrm{e}^{-\mathrm{j}\beta_g^{(2)}} & \cdots & \mathrm{e}^{-\mathrm{j}\beta_g^{(N_g)}} \end{pmatrix}. \tag{16b}$$

Eq. (16a) gives N_g-3 solutions for $\mathbf{s}_g$ as [5]

$$\mathbf{s}_g^{(k)} = (\mathrm{e}^{\mathrm{j}k\beta_g^{(1)}}, \mathrm{e}^{\mathrm{j}k\beta_g^{(2)}}, \ldots, \mathrm{e}^{\mathrm{j}k\beta_g^{(N_g)}})^T, \quad k = 2,3,\ldots,N_g-2. \tag{17}$$

These N_g-3 solutions form an orthogonal basis of the solution space [17,19]. Substitution of Eq. (17) into Eq. (14) gives the N_g-3 absorber mode eigenvectors with identical eigenvalue $\lambda = \mathrm{j}\Omega n_g$.

Substitution of $\lambda = -\mathrm{j}\Omega n_g$ into the three rotor equations in Eq. (5) also yields Eq. (16a). In this case we choose the N_g-3 solutions as the orthogonal vectors $\bar{\mathbf{s}}_g^{(k)}$. The corresponding eigenvectors from Eq. (14) are the complex conjugates of the eigenvectors based on the vectors $\mathbf{s}_g^{(k)}$ corresponding to $\lambda = \mathrm{j}\Omega n_g$. Therefore, each of the two complex conjugate eigenvalues $\lambda = \pm \mathrm{j}\Omega n_g$ has multiplicity N_g-3.

Based on Eqs. (14) and (17), the phases of the motions of adjacent absorbers within the group differ by $k \cdot 360^\circ/N_g$, where $k = 2,3,\ldots,N_g-2$, while the magnitudes are identical (see Fig. 4 where $k=2$). Thus, the phase indices of the absorber mode associated with the gth group are $k = 2,3,\ldots,N_g-2$. These are the same as for cyclically symmetric CPVA systems [5]. These are traveling wave modes [17].

For a group with unity tuning order $n_g = \sqrt{l_g/r_g} = 1$ the third equation of Eq. (16a) vanishes. This supplements the vector $\mathbf{s}_g^{(1)}$ to the solution space of the revised Eq. (16a), yielding the additional eigenvector

$$\boldsymbol{\phi} = (0,0,0,\mathbf{0}_{1\times N_1}, \mathbf{0}_{1\times N_2}, \ldots, \mathbf{0}_{1\times N_{g-1}}, \mathbf{s}_g^{(1)}, \mathbf{0}_{1\times N_{g+1}}, \ldots, \mathbf{0}_{1\times N_p})^T, \tag{18}$$

with eigenvalue $\lambda = \mathrm{j}\Omega$. This is also a solution of the translational mode eigenvalue problem in Eq. (12) for unity tuning order. Thus, Eq. (18) could be labeled as either an absorber mode (Eq. (14)) or a translational mode (Eq. (11)). The phase index of this eigensolution is $k=1$, however, identifying it as a translational mode rather than an absorber mode. Thus, the numbers of modes of each of the three mode types does not change when some absorber groups have unity tuning order.

3.5. Completeness of the vibration mode structure

According to the analytical derivations, there are $p+1$ pairs of complex conjugate rotational modes, $2(p+1)$ pairs of complex conjugate translational modes, and p pairs of complex conjugate absorber modes. Each of the p pairs of absorber modes associates with a group of absorbers. The eigenvalue multiplicity of the absorber mode associated with the gth group is N_g-3. Thus, the total number of pairs of all types is $\sum_{g=1}^{p} N_g + 3$, equalling the total number of degrees of freedom. Hence, there are no mode types other than rotational, translational, and absorber modes in the vibration mode structure.

None of the above derivations require any assumptions regarding the absorber numbers, masses, tuning orders, and relative spacing angles between the groups. Thus, the derived vibration mode structure holds for arbitrary properties of the multiple groups provided each group has identical, equally spaced absorbers.

Similar modal properties exist in compound planetary gears [20,21]. Other planetary gear systems also have modal properties similar to CPVA systems [16,22–26]. Similar modal properties occur in other cyclically symmetric systems such as rotationally periodic structures [27,28], spinning disks [18,29], and bladed disk assemblies [17,30–34].

3.6. Physical explanations of the vibration mode structure

For rotational modes, the absorbers in each group move identically. The absorbers belonging to different groups couple through the rotor. According to [5], each group of absorbers with identical motions exerts only net rotor moment but no net rotor force. The individual forces on the rotor from each absorber in the group cancel and the net rotor force vanishes. The net rotor moment from all of the groups balances with the rotor inertia in the equation of motion for rotor rotation. According to the equation governing rotor rotation in Eq. (8), the net moment that the gth group exerts on the rotor is

$$M_g = N_g m_g (l_g + r_g)\lambda^2[(l_g + r_g)\mu + s_g]\mathrm{e}^{\lambda t}. \tag{19}$$

Because the absorber modal deflections of the different groups are coupled through the rotor, the moment of the gth group in Eq. (19) is linked to the moments from other groups through the rotor rotation. The net rotor moment from all the absorbers is the summation of the moments in Eq. (19) for $g = 1,2,\ldots,p$. Thus, the net rotor moment varies with the eigenvalue and the mode. The net rotor moment is zero for the rigid body mode.

For translational modes, the absorbers in each group move with identical amplitudes. The phases of adjacent absorbers differ by $360^\circ/N_g$. Each group of absorbers that move with these properties exerts only net rotor force but no net rotor moment [5]. The net rotor force from all groups balances with the rotor linear momentum. From the equation that governs the rotor translation in Eq. (12), the force that the gth group exerts on the rotor in the $\mathbf{e}_1^0$ direction is

$$F_g = N_g m_g(\lambda - \mathrm{j}\Omega)^2(2x - \mathrm{j}s_g)\mathrm{e}^{\lambda t}. \tag{20}$$

Similar to the rotor moment of the gth group for rotational modes, the force in Eq. (20) depends on the eigenvalue and modal deflections of the rotor and the gth group. The force in the $\mathbf{e}_2^0$ direction is j times Eq. (20). The summation of the forces in Eq. (20) for $g=1,2,\ldots,p$ gives the total net rotor force in the $\mathbf{e}_1^0$ direction and similarly for $\mathbf{e}_2^0$. The total net rotor force rotates with respect to the rotating basis $(\mathbf{e}_1^0,\mathbf{e}_2^0)$ with a constant magnitude and frequency $-\mathrm{j}\lambda$ (a circle). Thus, if $\lambda=-\mathrm{j}\Omega$ (which is possible for translational modes), the total net rotor force becomes a fixed force in the fixed basis. Otherwise, it is a rotating force in the fixed basis as well as in the rotor-fixed basis. If the eigenvalue $\lambda=\mathrm{j}\Omega$, the net rotor force vanishes.

For absorber modes, only one group of absorbers moves, and the absorbers have identical amplitudes. The phases of adjacent absorbers differ by $k\cdot 360^\circ/N_g$, where $k=2,3,\ldots,N_g$. For general motions, the absorbers in different groups are connected through the rotor. For absorber modes, however, the absorbers exert no net moment or force on the rotor [5], removing any possible coupling between absorber groups. The motions of the active group of absorbers do not affect any of the other groups.

The net force and moment exerted on the rotor by the individual absorber groups can physically explain why the highly structured modal properties of systems with one group of absorbers remain when multiple groups are included, despite the apparent breaking of cyclic symmetry. Because of the cyclic symmetry, the rotational modes of a single-group system (with phase index $k=0$) are such that the absorbers exert a net moment but no net force on the rotor [5]. The addition of a second group of identical, equally spaced (i.e., cyclically symmetric when viewed separately from the existing group) absorbers moving with the properties of a rotational mode creates a second net rotor moment but no net force; this holds regardless of this group's relative angular spacing with the first group, its number of absorbers, and its absorber parameters. These two groups couple with the rotor rotation; there cannot be rotor translation in such a mode, however, because this would need to be balanced by absorber forces not possible when the absorbers move in the form of rotational modes. This physical argument shows only that it is possible (but not guaranteed) for both systems with both groups to have modes where each group has the features of a single-group rotational mode and the rotor has only rotation. The foregoing analytical derivations prove that this is in fact the modes that do occur. This pattern continues with the addition of additional groups, provided each group is cyclically symmetric. Thus, one obtains the eigenvalue problem Eq. (8) where each absorber group moves with the features of a single-group rotational mode and the multiple groups are coupled solely through rotor rotation. A similar argument can be made for the translational modes (with phase index $k=\pm 1$) for the transition from a single group of absorbers to multiple groups. That discussion involves net forces rather than net moments. For absorber modes, the absorbers have no coupling through the rotor because the absorbers exert no net force or moment on the rotor. In that case, it is expected that absorber modes of additional groups are completely uncoupled from each other and from rotational and translational modes.

From these results and prior experience with planetary gears, we speculate that this result generalizes to other systems having multiple groups of elements where each group is cyclically symmetric but the overall system is not. In that case, we expect modes of the single-group system with N_1 elements to have motions of the cyclically symmetric elements described by phase indices ranging from $0,\pm 1,2,\ldots,N_1-2$, as exist for CPVA systems [5], planetary gears [16,22–26], disk-spindle systems [18,29], and bladed disk assemblies [17,30–34]. When additional groups are added to form a multigroup system, the motions of the elements in the additional groups will have phase indices of $0,\pm 1,2,\ldots,N_g-2$, where N_g is the number of elements in the gth group. Modes with phase indices of 0, 1, and -1 will couple together into system modes [29]. Modes with other phase indices will have motions confined solely to degrees of freedom in one isolated group of cyclically symmetric elements. For modes with phase index of 0, any central (i.e., axisymmetric) elements, such as the rotor in CPVA systems or the sun and ring gears in planetary gears, will have rotation but no in-plane translation. For modes with phase index of ± 1, any central elements will have translation but no rotation about the axis of symmetry.

4. Stability

CPVA systems with one group of equally spaced, identical absorbers have a vanishing translational mode eigenvalue at a non-zero rotor speed that is defined as a critical speed, and they have complex eigenvalues with positive real parts (flutter instability) in some speed regions [5]. These stability issues are analyzed in this section for the more general current system.

4.1. Critical speeds

Critical speeds are non-zero speeds where an eigenvalue vanishes. From Eq. (5) with $\lambda=0$, the critical speeds Ω_c are obtained from

$$(\mathbf{K}_b-\Omega_c^2\mathbf{K}_\Omega)\boldsymbol{\phi}_c=\mathbf{0}. \tag{21}$$

Although Eq. (21) appears to be a standard self-adjoint eigenvalue problem with the critical speeds Ω_c as the eigenvalues, the matrix $\mathbf{K}_\Omega$ is singular. Therefore, the critical speeds and associated eigenvectors are obtained by solving for the null space of $\mathbf{K}_b-\Omega_c^2\mathbf{K}_\Omega$.

The absorber equations of Eq. (21) are

$$\Omega_c^2\left(m_g x\sin\beta_g^{(i)}-m_g y\cos\beta_g^{(i)}+m_g s_g^{(i)}\frac{l_g}{r_g}\right)=0,\quad i=1,2,\ldots,N_g,\quad g=1,2,\ldots,p. \tag{22}$$

Each of these equations has exactly two independent solutions that can be expressed as

$$x=1,\quad y=0,\quad s_g^{(i)}=-\frac{r_g}{l_g}\sin\beta_g^{(i)}, \tag{23a}$$

$$x=0,\quad y=1,\quad s_g^{(i)}=\frac{r_g}{l_g}\cos\beta_g^{(i)}, \tag{23b}$$

$$i=1,2,\ldots,N_g,\quad g=1,2,\ldots,p. \tag{23c}$$

Therefore, a basis of the null space of $\mathbf{K}_b-\Omega_c^2\mathbf{K}_\Omega$ is formed by vectors that satisfy Eq. (23)

$$\boldsymbol{\phi}_c^{(1)}=(\boldsymbol{\phi}_r^{(1)},\boldsymbol{\phi}_1^{(1)},\boldsymbol{\phi}_2^{(1)},\ldots,\boldsymbol{\phi}_p^{(1)})^T, \tag{24a}$$

$$\boldsymbol{\phi}_c^{(2)}=(\boldsymbol{\phi}_r^{(2)},\boldsymbol{\phi}_1^{(2)},\boldsymbol{\phi}_2^{(2)},\ldots,\boldsymbol{\phi}_p^{(2)})^T, \tag{24b}$$

$$\boldsymbol{\phi}_r^{(1)}=(1,0,0)^T,\quad \boldsymbol{\phi}_g^{(1)}=-\left(\frac{r_g}{l_g}\sin\beta_g^{(1)},\frac{r_g}{l_g}\sin\beta_g^{(2)},\ldots,\frac{r_g}{l_g}\sin\beta_g^{(N_g)}\right)^T, \tag{24c}$$

$$\boldsymbol{\phi}_r^{(2)}=(0,1,0)^T,\quad \boldsymbol{\phi}_g^{(2)}=\left(\frac{r_g}{l_g}\cos\beta_g^{(1)},\frac{r_g}{l_g}\cos\beta_g^{(2)},\ldots,\frac{r_g}{l_g}\cos\beta_g^{(N_g)}\right)^T. \tag{24d}$$

Substitution of the two vectors in Eq. (24) into each of the rotor translation equations in Eq. (21) both yield the critical speed

$$\Omega_c=\sqrt{\frac{k_r}{m_r+\sum_{g=1}^{p}N_g m_g\left(1+\frac{r_g}{2l_g}\right)}}. \tag{25}$$

The rotor rotation equation in Eq. (21) is a trivial equation ($0=0$) that is automatically satisfied and does not affect the critical speed.

Because Eq. (21) is a special case of Eq. (5), the critical speed eigensolutions must have the previously derived modal properties. The critical speed eigenvectors in Eq. (24) are real-valued, consistent with the symmetric matrices in Eq. (21). Linear combinations of these vectors form another basis of the null space of $\mathbf{K}_b-\Omega_c^2\mathbf{K}_\Omega$ as

$$\boldsymbol{\phi}_c=(\boldsymbol{\phi}_r,\boldsymbol{\phi}_1,\boldsymbol{\phi}_2,\ldots,\boldsymbol{\phi}_p)^T, \tag{26a}$$

$$\overline{\boldsymbol{\phi}}_c=(\overline{\boldsymbol{\phi}}_r,\overline{\boldsymbol{\phi}}_1,\overline{\boldsymbol{\phi}}_2,\ldots,\overline{\boldsymbol{\phi}}_p)^T, \tag{26b}$$

$$\boldsymbol{\phi}_r=(1,\mathrm{j},0)^T,\quad \boldsymbol{\phi}_g=\mathrm{j}\frac{r_g}{l_g}(e^{\mathrm{j}\beta_g^{(1)}},e^{\mathrm{j}\beta_g^{(2)}},\ldots,e^{\mathrm{j}\beta_g^{(N_g)}})^T,\quad g=1,2,\ldots,p. \tag{26c}$$

The two vectors in Eqs. (24a) and (24b) are the real and imaginary parts of the vector in Eq. (26a), respectively. Expressed in the form Eq. (26), the two critical speed eigenvectors are a pair of complex conjugate translational modes in the form of Eq. (11) within a normalization factor. The critical speed in Eq. (25) is associated with the pair of translational modes in Eq. (26).

The absorber mode eigenvalues in Eq. (15) vanish only at zero rotor speed, so absorber modes do not have critical speeds.

Because $\mathbf{K}_b\boldsymbol{\phi}_c=\mathbf{0}$ and $\mathbf{K}_\Omega\boldsymbol{\phi}_c\neq\mathbf{0}$ for all non-rigid body rotational modes, substitution of the rotational mode eigenvector in Eq. (7) into Eq. (21) yields $\Omega_c=0$ except for the rigid body mode that is present at any speed and not related to critical speeds. Thus, no rotational modes experience critical speeds at non-zero rotor speeds.

Exactly one non-zero critical speed associated with a pair of complex conjugate translational modes exists. According to Eq. (25), all groups of absorbers affect this non-zero critical speed. The use of more groups results in a smaller critical speed.

4.2. Flutter instability

Flutter instability where a complex eigenvalue λ has positive real part occurs if and only if the discriminant in Eq. (6), $\Delta=-\tilde{g}^2-4\tilde{m}\tilde{k}$, is positive.

A necessary but not sufficient condition for flutter is that one and only one of $\tilde{m}$ and $\tilde{k}$ is negative. $\tilde{m}$ is positive for all three mode types, and $\tilde{k}$ is non-negative for both rotational and absorber modes. Thus, no rotational or absorber modes experience flutter instability.

For rotor speeds less than the non-zero critical speed, Eq. (25) gives

$$k_r \geq \left[m_r + \sum_{g=1}^{p} N_g m_g \left(1 + \frac{r_g}{2 l_g} \right) \right] \Omega^2. \tag{27}$$

When Eq. (27) is satisfied, $\tilde{k}$ is non-negative for any translational mode. This ensures that no flutter instability occurs below the critical speed.

When the rotor speed exceeds the critical speed, calculation of the discriminant Δ for a translational mode yields

$$\Delta = -8k_r|x|^2 \left[\left(2m_r + \sum_{g=1}^{p} N_g m_g \right) |x|^2 + \sum_{g=1}^{p} N_g m_g |jx + s_g|^2 \right] - \left(2\Omega \sum_{g=1}^{p} N_g m_g |s_g|^2 \right)^2 + 4\Omega^2 \sum_{g=1}^{p} N_g m_g \left(1 - \frac{l_g}{r_g} \right) |s_g|^2 \left[\left(2m_r + \sum_{g=1}^{p} N_g m_g \right) |x|^2 + \sum_{g=1}^{p} N_g m_g |jx + s_g|^2 \right]. \tag{28}$$

Δ in Eq. (28) can be positive only when at least one group of absorbers has tuning order $n_g = \sqrt{l_g / r_g} < 1$. Having $n_g < 1$ for one or more groups is only a necessary, but not sufficient flutter criterion in this derivation. From a range of numerical simulations, however, all systems having at least one $n_g < 1$ experience flutter.

4.3. Numerical examples

Fig. 5 shows the eigenvalues of the CPVA system with three groups of absorbers described in Table 4. Only the positive parts are plotted because the real and imaginary loci are symmetric about the rotor speed axis. Systems with arbitrary spacing angles between the three groups yield eigenvalue loci identical to those in Fig. 5.

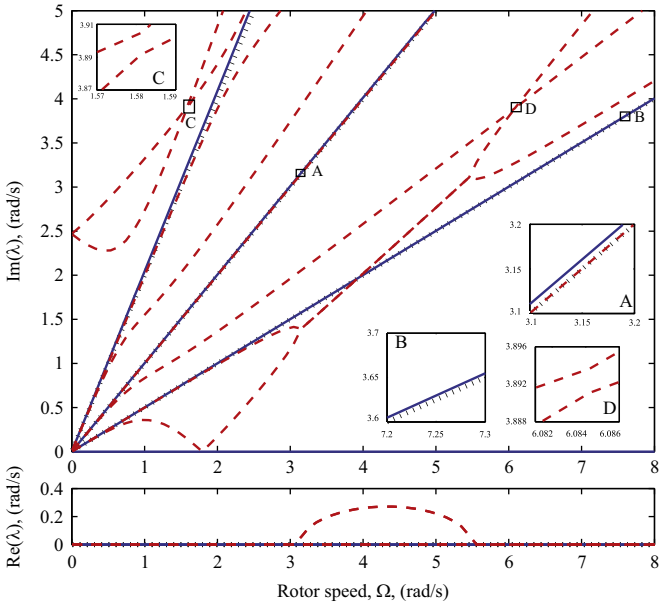

Fig. 5. Real and imaginary parts of eigenvalues of the CPVA system with three groups of absorbers given in Table 4 for varying rotor speed. The results do not depend on the relative spacing between groups. Absorber modes are shown by dotted (black) lines, rotational modes are shown by solid (blue) lines, and translational modes are shown by dashed (red) lines. The inset figures zoom in on the highlighted regions A, B, C, and D. (For interpretation of the references to color in this figure legend, the reader is referred to the web version of this article.)

Table 4
Parameters of a CPVA example system used to examine the critical speeds and flutter instability.

Parameter	First group	Second group	Third group
Rotor mass, m_r (kg)		11	
Rotor translational stiffness, k_r (N/m)		100	
Number of absorbers	4	4	4
Absorber mass, m (kg)	0.9	0.9	0.9
Distance between center and pivot, l (m)	0.0025	0.01	0.04
Absorber radius, r (m)	0.01	0.01	0.01

There is only one non-zero critical speed in Fig. 5, and it is the translational mode critical speed at 1.8 rad/s that equals the value from Eq. (25).

The imaginary loci of the two smallest translational mode eigenvalues coincide between 3.0 rad/s and 5.5 rad/s. The real loci of these eigenvalues are non-zero, and one of them is positive within this range. Thus, one of these translational mode eigenvalues experiences flutter instability. Flutter instability occurs in this system because the first group has tuning order $n_1 = 1/2$ that is less than unity. If the first group is eliminated, no flutter instability occurs.

Like the axisymmetric gyroscopic systems of spinning disks [35–37], spinning shafts [38], and disk-spindle systems [39,40], the imaginary parts of the two initially degenerate non-zero translational mode eigenvalues split at zero rotor speed. One of them increases while the other decreases. The imaginary parts of the four initially zero degenerate translational mode eigenvalues also split, but, unlike the behavior above, all of them increase as the rotor speed increases near the zero rotor speed. This behavior is similar to that of cyclically symmetric CPVA systems [5].

The enlarged figure of region A shows that a translational mode locus coincides with an absorber mode locus. This is because of the unity tuned group (the second group in Table 4). The smallest non-rigid body rotational mode locus in the imaginary part of Fig. 5 appears to overlap with the smallest absorber mode locus, but the enlarged figure of region B shows that they do not coincide with each other. The close proximity of these eigenvalues of different types may relate to natural frequency clusters that occur in planetary gears [41].

The enlargements of regions C and D in Fig. 5 show the veering of two translational mode loci near $\Omega = 1.6$ rad/s and $\Omega = 6.1$ rad/s. Fig. 5 also shows the lowest translational mode locus crosses the rotational and absorber mode loci near $\Omega = 4.0$ rad/s. Loci of the same mode type veer, while loci of different mode types cross each other. These behaviors are similar to planetary gear systems [16,42,43].

5. Conclusions

This paper investigates the symmetry breaking effects on the modal properties of CPVA systems when multiple groups of absorbers are used. Each group of absorbers is a set of equally spaced, identical absorbers. The cyclically symmetric properties remain within each group, but the entire system is not cyclically symmetric. Surprisingly perhaps, this symmetry breaking does not destroy the well-defined mode structure for single-group CPVA systems. The main results are:

1. The eigenspace decomposition of the system into rotational, translational, and absorber modes results from the cyclic symmetry of each group and holds for arbitrary relative angular spacing between the multiple groups. A physical explanation of the forces and moments that the individual groups exert on the rotor gives insight into this finding.
2. There are $p+1$ pairs of complex conjugate rotational modes, $2(p+1)$ pairs of complex conjugate translational modes, and p pairs of complex conjugate absorber modes in the vibration mode structure. No other mode types are possible. Each absorber mode with eigenvalue multiplicity N_g-3 associates with the gth group. The absorber modes exist only when more than three absorbers are used in the associated group.
3. The absorber groups couple through the rotor rotation and translation for rotational and translational modes, respectively, and are independent of each other for absorber modes.
4. There is exactly one non-zero critical speed, and it is associated with a pair of complex conjugate translational modes. The use of more groups results in a smaller critical speed.
5. Only the translational modes experience flutter instability, and this occurs only when at least one group of absorbers has tuning order less than unity. The instability speed range is above the non-zero critical speed.

References

[1] C. Shi, R.G. Parker, S.W. Shaw, Tuning of centrifugal pendulum vibration absorbers for translational and rotational vibration reduction, Mechanism and Machine Theory, in press, http://dx.doi.org/10.1016/j.mechmachtheory.2013.03.004.
[2] B.J. Vidmar, S.W. Shaw, B.F. Feeny, B.K. Geist, Analysis and design of multiple order centrifugal pendulum vibration absorbers, *ASME 2012 International Design Engineering Technical Conferences and Computers and Information in Engineering Conference*, No. DETC2012-71074, Chicago, Illinois, USA, 2012.
[3] C.-P. Chao, S.W. Shaw, C.-T. Lee, Stability of the unison response for a rotating system with multiple tautochronic pendulum vibration absorbers, *Journal of Applied Mechanics* 64 (1) (1997) 149–156.
[4] C.-P. Chao, C.-T. Lee, S.W. Shaw, Non-unison dynamics of multiple centrifugal pendulum vibration absorbers, *Journal of Sound and Vibration* 204 (5) (1997) 769–794.
[5] C. Shi, R.G. Parker, Modal properties and stability of centrifugal pendulum vibration absorber systems with equally spaced, identical absorbers, *Journal of Sound and Vibration* 331 (21) (2012) 4807–4824.
[6] C.-P. Chao, S.W. Shaw, The dynamic response of multiple pairs of subharmonic torsional vibration absorbers, *Journal of Sound and Vibration* 231 (2) (2000) 411–431.
[7] A.S. Alsuwaiyan, S.W. Shaw, Steady-state responses in systems of nearly-identical vibration absorbers, *Journal of Vibration and Acoustics* 125 (1) (2003) 80–87.
[8] A.S. Alsuwaiyan, S.W. Shaw, Localization of free vibration modes in systems of nearly-identical vibration absorbers, *Journal of Sound and Vibration* 228 (3) (1999) 703–711.
[9] D.L. Cronin, Shake reduction in an automobile engine by means of crankshaft-mounted pendulums, *Mechanism and Machine Theory* 27 (5) (1992) 517–533.
[10] O.A. Bauchau, J. Rodriguez, S.-Y. Chen, Modeling the bifilar pendulum using nonlinear, flexible multibody dynamics, *Journal of the American Helicopter Society* 48 (1) (2003) 53–62.

[11] H.H. Denman, Tautochronic bifilar pendulum torsion absorbers for reciprocating engines, *Journal of Sound and Vibration* 159 (2) (1992) 251–277.
[12] W. Miao, T. Mouzakis, Bifilar Analysis Study, Vol. 1, Tech. Rep. NASA-CR-159227, NASA, 1980.
[13] R. Sopher, R.E. Studwell, S. Carssarino, S.P.R. Kottapalli, Coupled Rotor/Airframe Vibration Analysis, Tech. Rep. NASA-CR-3582, NASA, 1982.
[14] R.J. Monroe, S.W. Shaw, A.H. Haddow, B.K. Geist, Accounting for roller dynamics in the design of bifilar torsional vibration absorbers, *Journal of Vibration and Acoustics* 133 (6) (2011). 061002-1-10.
[15] L. Meirovitch, A new method of solution of the eigenvalue problem for gyroscopic systems, *AIAA Journal* 12 (10) (1974) 1337–1342.
[16] C.G. Cooley, R.G. Parker, Vibration properties of high-speed planetary gears with gyroscopic effects, *Journal of Vibration and Acoustics* 134 (6) (2012). 061014-1-11.
[17] B.J. Olson, Order-Tuned Vibration Absorbers for Systems with Cyclic Symmetry with Applications to Turbomachinery, PhD Thesis, Michigan State University, East Lansing, Michigan, 2006.
[18] H. Kim, I.Y. Shen, Ground-based vibration response of a spinning, cyclic, symmetric rotor with gyroscopic and centrifugal softening effects, *Journal of Vibration and Acoustics* 131 (2) (2009). 021007-1-13.
[19] G.S. Ottarsson, Dynamic Modeling and Vibration Analysis of Mistuned Bladed Disks, PhD Thesis, University of Michigan, Ann Arbor, Michigan, 1994.
[20] Y. Guo, R.G. Parker, Purely rotational model and vibration modes of compound planetary gears, *Mechanism and Machine Theory* 45 (3) (2010) 365–377.
[21] D.R. Kiracofe, R.G. Parker, Structured vibration modes of general compound planetary gear systems, *Journal of Vibration and Acoustics* 129 (1) (2007) 1–16.
[22] J. Lin, R.G. Parker, Analytical characterization of the unique properties of planetary gear free vibration, *Journal of Vibration and Acoustics* 121 (3) (1999) 316–321.
[23] J. Lin, R.G. Parker, Structured vibration characteristics of planetary gears with unequally spaced planets, *Journal of Sound and Vibration* 233 (5) (2000) 921–928.
[24] T. Eritenel, R.G. Parker, Modal properties of three-dimensional helical planetary gears, *Journal of Sound and Vibration* 325 (1–2) (2009) 397–420.
[25] X. Wu, R.G. Parker, Modal properties of planetary gears with an elastic continuum ring gear, *Journal of Applied Mechanics* 75 (3) (2008). 031014-1-12.
[26] R.G. Parker, X. Wu, Vibration modes of planetary gears with unequally spaced planets and an elastic ring gear, *Journal of Sound and Vibration* 329 (11) (2010) 2265–2275.
[27] I.-Y. Shen, Vibration of rotationally periodic structures, *Journal of Sound and Vibration* 172 (4) (1994) 459–470.
[28] H. Kim, I.-Y. Shen, Vibration of a spinning rotationally periodic rotor, *ASME 2007 International Design Engineering Technical Conferences and Computers and Information in Engineering Conference*, No. DETC2007-34888, Las Vegas, Nevada, USA, 2007.
[29] H. Kim, N.T. Khalid Colonnese, I.Y. Shen, Mode evolution of cyclic symmetric rotors assembled to flexible bearings and housing, *Journal of Vibration and Acoustics* 131 (5) (2009). 051008-1-9.
[30] O.O. Bendiksen, Mode localization phenomena in large space structures, *AIAA Journal* 25 (9) (1987) 1241–1248.
[31] S.B. Chun, C.W. Lee, Vibration analysis of shaft-bladed disk system by using substructure synthesis and assumed modes method, *Journal of Sound and Vibration* 189 (5) (1996) 587–608.
[32] D.J. Ewins, Vibration characteristics of bladed disc assemblies, *Journal of Mechanical Engineering Science* 15 (3) (1973) 165–186.
[33] D.J. Ewins, Vibration modes of mistuned bladed disks, *American Society of Mechanical Engineers, Gas Turbine Conference and Products Show*, Houston, Texas, USA, 1975.
[34] H. Irretier, Spectral analysis of mistuned bladed disk assemblies by component mode synthesis, *ASME 1983 International Design Engineering Technical Conferences and Computers and Information in Engineering Conference*, Dearborn, Michigan, USA, 1983, pp. 115–125.
[35] S.A. Tobias, R.N. Arnold, The influence of dynamical imperfection on the vibration of rotating disks, *Journal of Mechanical Engineering Science* 171 (1959) 669–690.
[36] C.D. Mote Jr., Stability of circular plates subjected to moving loads, *Journal of the Franklin Institute* 290 (4) (1970) 329–344.
[37] J.S. Chen, D.B. Bogy, Effects of load parameters on the natural frequencies and stability of a flexible spinning disk with a stationary load system, *Journal of Applied Mechanics* 59 (2) (1992) S230–S235.
[38] R.P.S. Han, J.W.-Z. Zhu, Modal analysis of rotating shafts: *a body-fixed axis formulation approach*, *Journal of Sound and Vibration* 156 (1) (1992) 1–16.
[39] R.G. Parker, P.J. Sathe, Free vibration and stability of a spinning disk-spindle system, *Journal of Vibration and Acoustics* 121 (3) (1999) 391–396.
[40] R.G. Parker, P.J. Sathe, Exact solutions for the free and forced vibration of a rotating disk-spindle system, *Journal of Sound and Vibration* 223 (3) (1999) 445–465.
[41] T. Ericson, R.G. Parker, Natural frequency clustering in planetary gears, *ASME 2012 International Design Engineering Technical Conferences and Computers and Information in Engineering Conference*, No. DETC2012-71501, Chicago, Illinois, USA, 2012.
[42] J. Lin, R.G. Parker, Natural frequency veering in planetary gears, *Mechanics of Structures and Machines* 29 (4) (2001) 411–429.
[43] C. G. Cooley, R. G. Parker, Critical speeds, divergence, and flutter instability in planetary gears, *ASME 2012 International Design Engineering Technical Conferences and Computers and Information in Engineering Conference*, No. DETC2012-70935, Chicago, Illinois, USA, 2012.